

9-1996

Cross Sections for the Production of He⁺ (np) 2P0 States by 50 to 150 keV Proton Impact on Helium

Wayne C. Stolte

University of Nevada, Las Vegas, wcstolte@lbl.gov

R. Bruch

University of Nevada, Reno, bruch@unr.edu

Follow this and additional works at: https://digitalscholarship.unlv.edu/chem_fac_articles



Part of the [Analytical Chemistry Commons](#), [Atomic, Molecular and Optical Physics Commons](#), [Biological and Chemical Physics Commons](#), [Elementary Particles and Fields and String Theory Commons](#), and the [Physical Chemistry Commons](#)

Repository Citation

Stolte, W. C., Bruch, R. (1996). Cross Sections for the Production of He⁺ (np) 2P0 States by 50 to 150 keV Proton Impact on Helium. *Physical Review A*, 54(3), 2116-2120.

https://digitalscholarship.unlv.edu/chem_fac_articles/43

This Article is protected by copyright and/or related rights. It has been brought to you by Digital Scholarship@UNLV with permission from the rights-holder(s). You are free to use this Article in any way that is permitted by the copyright and related rights legislation that applies to your use. For other uses you need to obtain permission from the rights-holder(s) directly, unless additional rights are indicated by a Creative Commons license in the record and/or on the work itself.

This Article has been accepted for inclusion in Chemistry and Biochemistry Faculty Publications by an authorized administrator of Digital Scholarship@UNLV. For more information, please contact digitalscholarship@unlv.edu.

Cross sections for the production of excited He^+ (np) $^2P^o$ states by 50–150-keV proton impact on helium

W. C. Stolte and R. Bruch

Department of Physics, University of Nevada, Reno, Nevada 89557-0058

(Received 19 September 1995)

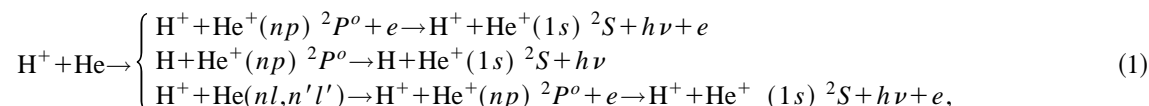
Cross sections have been measured for the production of He^+ (np) $^2P^o$ states, $n=2,3,4$, by proton impact on helium over a projectile velocity range of 1.42–2.45 a.u. ($50 \leq E \leq 150$ keV). Cross sections were determined by measuring the extreme ultraviolet photons emitted from excited He^+ ions. The data indicate a lower energy than expected for the maximum cross section. A comparison of the present results in terms of projectile energy dependence with the cross sections for excitation to He ($1snp$) $^1P^o$, ionization, and total electron capture suggests the primary mechanism for the production of excited He^+ at low energies is transfer excitation, with ionization excitation being the dominant mechanism at higher energies. [S1050-2947(96)04509-X]

PACS number(s): 34.50.Fa

I. INTRODUCTION

Ionization excitation and other two-electron processes involving simple atoms, such as helium, have been the focus of many studies over the past several years [1–11]. In this work

extreme ultraviolet (EUV) cross-section measurements are presented for excitation of helium from the ground state to ($2p$) $^2P^o$, ($3p$) $^2P^o$, and ($4p$) $^2P^o$ states following 50–150-keV proton impact. These states can be principally formed by the following reaction channels:



which are, respectively, ionization excitation, transfer excitation, and double excitation with subsequent autoionization to an excited He^+ (np) $^2P^o$ state, all of which can then decay via an electric dipole transition.

Previously there has been no detailed investigation of these processes in this energy range, and most earlier studies have focused on the ($2p$) $^2P^o \rightarrow (1s) \ ^2S$ transition, resulting in a lack of data for higher Rydberg levels [2,3,5]. The energy range chosen and the processes measured are of great importance in the study of collisional dynamics [1,11] and for plasma diagnostics in fusion reactor design [12–14]. Measurements of two-electron processes such as ionization excitation and/or transfer excitation are especially important to the understanding of electron-electron correlation [1]. The measured processes are also important for plasma diagnostics when a neutral helium beam is passed through a plasma in a tokamak fusion reactor to determine the plasma density [14]. It is necessary to know how much energy the beam loses due to atomic processes with the plasma protons and any impurities.

The present work represents detailed EUV results for the production of excited He^+ by proton impact in the intermediate velocity range. To our knowledge the only measurements for excited He^+ are those of Bailey *et al.* [2] for He^+ (np) $^2P^o$, $n=2-5$, states for 50-, 100-, and 156-keV proton impact, Schartner, Lommel, and Detleffsen [3] for the ($2p$) $^2P^o$ state for 75, 100, 125, and 150 keV, and a series of

measurements for ($2p$) $^2P^o$ and ($3p$) $^2P^o$ ranging from 15 to 35 keV performed by van Eck [15]. Comparison of the present work and all previous results shows reasonably good agreement (within 20%).

II. EXPERIMENT

In this experiment an apparatus was designed and constructed to study EUV fluorescence from an excited He^+ target by applying a high-resolution EUV spectroscopy technique. This experimental setup is similar to that described by Bailey *et al.* [2] and Bruch *et al.* [16]. In brief, positive-ion projectiles were provided by an electrostatic accelerator capable of producing mainly singly charged projectiles with energies ranging from about 50 to 150 keV. The projectile beam was then focused, steered, mass-charge selected, and directed towards the target chamber. Due to the low intensity of the measured spectral lines a differentially pumped gas cell was used to allow higher operating target pressures (30 mtorr) while still observing single-collision conditions. The target pressure was measured with a factory calibrated capacitance manometer. Stable target pressures with an uncertainty of 1% were achieved with a feedback control system [18]. The projectile ion was passed through the interaction region of the target cell and collected in a Faraday cup where the current was measured in order to normalize the resulting spectrum with respect to the projectile charge. Typical beam

currents for the projectiles used in this study were between 1 and 5 μA . A high-resolution 2.2-m grazing incidence monochromator (McPherson model 247) measured the emitted photons. This monochromator was positioned at right angles to the projectile beam and the EUV photons were counted with a Channel electron multiplier. Data acquisition has been accomplished by means of a computer automated measurement and control (CAMAC) system which adjusted the wavelength of the monochromator, accumulated photon counts and normalized them to the collected ion charge [19].

III. CROSS-SECTION EVALUATION

The evaluation of a cross section from the measured spectral line intensity was performed using the following equation [17]:

$$\sigma = \left(\frac{4\pi}{\omega} \right) \left(\frac{qe}{Q} \right) \frac{I(\lambda)}{K(\lambda)NLB} P - \sum_{k>i} \sigma_k A_{ki}, \quad (2)$$

where ω is the solid angle of acceptance for the monochromator, q the charge state of the projectile, e the electron charge, Q the charge normalization or the integrated beam charge, $I(\lambda)$ the measured line intensity, $K(\lambda)$ the detection sensitivity, N the target number density, L the target length, B the branching ratio of the transition investigated, P a correction for polarization effects, and $\sum_{k>i} \sigma_k A_{ki}$ represents the cascade correction.

To estimate the necessary cascade correction the procedure is as follows: one must first measure the emission cross sections for all of the cascading levels that contribute significantly to the population in the level of interest. Fortunately in this work, known branching ratios relate most of the cross sections for the cascading levels so that only a few cross sections are required. On the other hand, emission cross sections for He^+ (ns) 2S –(np) $^2P^o$ and (nd) $^2D^o$ –(np) $^2P^o$ have not been previously measured, to our knowledge, so the measured ($1s$) 2S –(np) $^2P^o$ results must be used to estimate the cascade effect. Several assumptions were applied, the first being that the population ratios of $3S$, $3P$, and $3D$ states observed in collision-induced excitation of hydrogen [20,21] are similar to the excited He^+ levels. Then we extended these population ratios from $n=3$ to $n=4, 5$, and 6 , by the use of an n^{-3} dependence. Dipole transitions are assumed to be the primary source of cascade feeding; therefore the F levels and any higher P levels contribute a negligible amount. The estimated cross sections can then be used to calculate the cascade contribution by use of the branching ratios.

For cascade feeding into the ($2p$) $^2P^o$ level, the following example is given:

$$\sum_{k>i} \sigma_k A_{ki} = \sum_{n>2} [\sigma(nS)A(nS-2P)\tau_{nS} + \sigma(nD)A(nD-2P)\tau_{nD}], \quad (3)$$

where σ_k , $\sigma(nS)$, and $\sigma(nD)$ are the excitation cross sections for the cascading levels; A_{ki} , $A(nS-2P)$, and $A(nD-2P)$, are the branching ratios relating the various levels, and τ_{nS} and τ_{nD} are the lifetimes of the levels. This very coarse approximation shows a high sensitivity of the correc-

TABLE I. Estimated cascade corrections (in units of 10^{-19} cm^2) for He^+ (np) $^2P^o$ transitions.

Energy (keV)	Cascade into ($2p$) $^2P^o$	Cascade into ($3p$) $^2P^o$	Cascade into ($4p$) $^2P^o$
50	9.3	0.93	0.16
60	7.7	0.91	0.16
70	6.6	0.74	0.13
80	5.3	0.60	0.10
90	5.3	0.63	0.11
95	5.3	0.61	0.11
100	5.0	0.52	0.093
105	4.6	0.57	0.10
110	4.1	0.45	0.080
115	3.8	0.52	0.092
120	3.7	0.36	0.064
125	3.4	0.35	0.063
130	3.3	0.37	0.065
156	2.4	0.22	0.046

tion to the estimated (nd) $^2D^o$ level cross sections. Also the small value of the branching ratios, in most instances, for the (ns) 2S levels causes the correction to be less sensitive to cascading from an S level. Table I gives the estimated cross-section corrections calculated for cascading into the ($2p$) $^2P^o$, ($3p$) $^2P^o$, and ($4p$) $^2P^o$ levels due to dipole transitions from higher levels. Previous estimates for cascading into ($2p$) $^2P^o$ for hydrogen are approximately 10% [20], and are estimated to be substantially larger for ionization excitation of helium by electron impact [4].

IV. RESULTS AND DISCUSSION

The measured cross sections for the production of excited He^+ states by proton impact on helium are presented in Table II and Fig. 1. The cross-section measurements were placed on an absolute scale at 100-keV projectile energy by comparison to the measured cross sections of Bailey *et al.* [2], then estimates for cascade contributions to each state selective cross section were applied. Total error includes statistical and fitting errors along with estimates of any instrumental errors. Error due to normalizing the present data to previous measurements contributes 15.1–15.7 % for the measurements by Bailey *et al.* and an additional 27.5% for their normalization cross section [2], resulting in a total normalization error of approximately 31%. For comparison the results of Bailey *et al.* [2], Schartner, Lommel, and Detleffsen [3], and the low-energy results from van Eck [15] are shown. From these data it is evident that the established cross-section curve has a maximum between about 35 and 50 keV for the ($2p$) $^2P^o$ and ($3p$) $^2P^o$ states.

In the intermediate-energy range, more than one process may contribute to the observed cross section; for example, excitation of the helium atom in addition to electron capture by the proton and ionization excitation. To elucidate this question in more detail an interesting comparison has been made between the processes of ionization, electron capture, excitation, and ionization excitation for the $\text{H}^+ + \text{He}$ collision system. The variation of cross sections with projectile energy

TABLE II. EUV cross sections (in units of $10^{-19} \text{ cm}^2/\text{atom}$) for $\text{He}^+ (np)^2P^o \rightarrow (1s)^2S$, $n=2-4$, transitions by proton impact on helium. The error shown includes statistical, fitting, and systematic errors. To calculate the total error, normalization errors of 31.4%, 31.5%, and 31.7% should be added to the respective $(2p)^2P^o$, $(3p)^2P^o$, and $(4p)^2P^o$ errors.

Energy (keV/amu)	$(2p)^2P^o$	$(3p)^2P^o$	$(4p)^2P^o$
50	49.8 ± 5.8	4.89 ± 0.77	1.52 ± 0.25
60	42.1 ± 5.0	3.61 ± 0.53	1.49 ± 0.31
70	35.9 ± 4.3	3.23 ± 0.44	1.21 ± 0.20
80	32.3 ± 3.8	2.55 ± 0.34	0.99 ± 0.20
90	26.5 ± 3.3	2.50 ± 0.35	1.04 ± 0.17
95	30.8 ± 3.5	2.58 ± 0.33	1.01 ± 0.17
100	24.8 ± 3.0	2.53 ± 0.39	0.86 ± 0.14
105	25.1 ± 2.9	2.13 ± 0.27	0.93 ± 0.15
110	21.0 ± 2.4	2.08 ± 0.28	0.74 ± 0.12
115	21.0 ± 2.5	1.59 ± 0.21	0.85 ± 0.14
120	21.7 ± 2.6	1.97 ± 0.27	0.59 ± 0.13
125	19.2 ± 2.1	1.76 ± 0.26	0.58 ± 0.13
130	18.6 ± 2.3	1.64 ± 0.25	0.60 ± 0.10
140	19.3 ± 2.4		

for the excitation to the $\text{He} (1s2p)^1P^o$ level [22–24] and the results for the production of the $\text{He}^+ (2p)^2P^o$ state are displayed in Fig. 2. In addition, the variation with impact energy of the ionization [25] and total electron-capture [12]

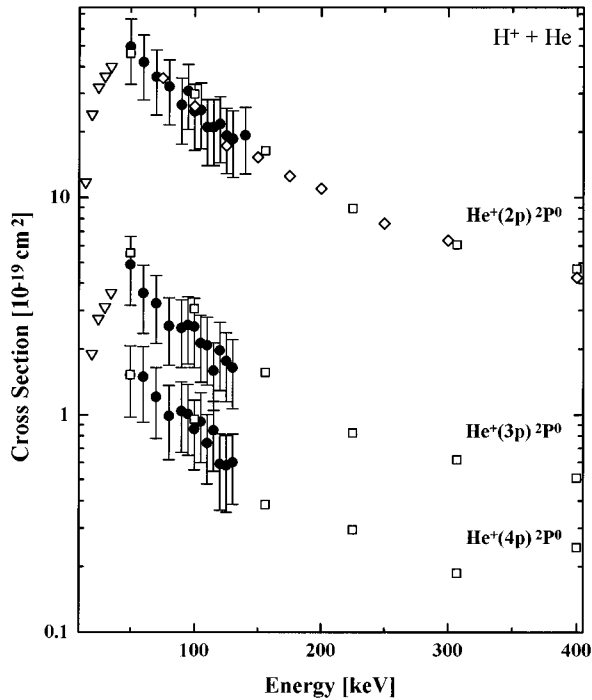


FIG. 1. Comparison of the present results, ●, for excitation to $\text{He}^+ (np)^2P^o$, $n=2-4$, states due to proton impact on helium (see text for error analysis), with previous measurements by Bailey *et al.* [2], □, Schartner, Lommel, and Detleffsen [3], ◇, and van Eck [15], ▽. Present results were normalized to those of Bailey *et al.* at 100 keV then corrected for cascade contributions; all previous results were not corrected for cascade contributions.

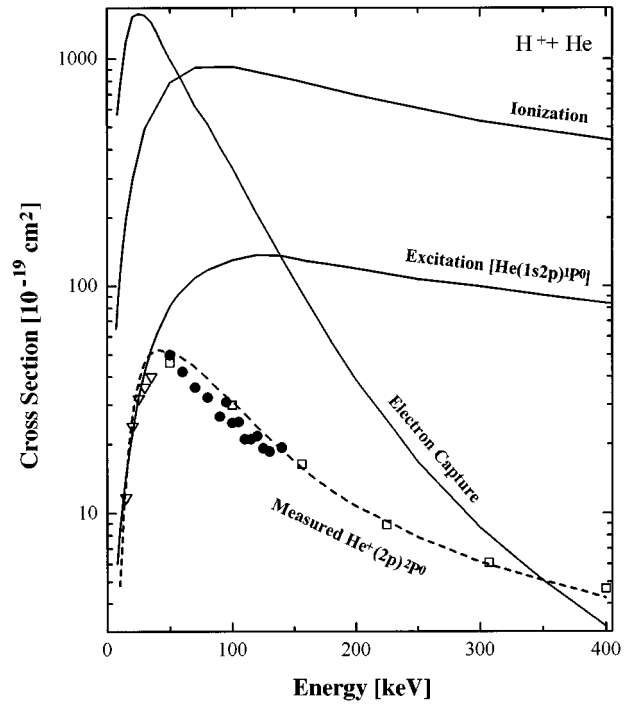


FIG. 2. Variation of cross sections for the production of $\text{He}^+ (2p)^2P^o$ with projectile energy. The ionization [25], total electron capture [11], and excitation cross sections for $\text{He} (1s2p)^1P^o$ [22–24] are included for comparison. The heavy dashed line passing through the measured, excited He^+ data represents a linear combination of the various cross-section products for excitation, ionization, and capture (see text). Present results, ●, cascade corrected, and those of Bailey *et al.* [2], □, and van Eck [15], ▽, neither of which have been corrected for cascade contributions, are included for comparison.

cross sections are plotted for comparison. The cross-section curve representing the ionization process and the curve defined by the measured excitation cross sections have similar energy dependencies. Likewise, the curve representing the change with impact energy of the total capture cross sections is similar to that measured for ionization excitation, especially below 200 keV. Another remarkable result of this comparison is that the cross sections for excitation to $\text{He} (1s2p)^1P^o$ states and ionization excitation to $\text{He}^+ (2p)^2P^o$ are of comparable magnitude for impact energies less than 50 keV (see Fig. 2). A theoretical investigation of this interesting effect may shed more light on the few-body collision dynamics and the threshold behavior of these types of collision processes.

In Figs. 3 and 4 we present the corresponding data for the higher n levels. The trend is very similar for the $n=3$ and 4 states, but it appears that the maxima are shifted slightly to lower energies. As can be seen from Figs. 2, 3, and 4 the cross sections decrease rapidly as a function of energy for the $\text{He}^+ (np)^2P^o$ states, whereas for the $\text{He} (1snp)^1P^o$ states the decrease is much less pronounced. In this connection we note that at 400-keV-impact energy the cross sections associated with $\text{He}^+ (2p)^2P^o$ are approximately 180 times smaller when compared to excitation of $\text{He} (1s2p)^1P^o$ at equal projectile velocities.

Additional insight into the collision mechanisms may be

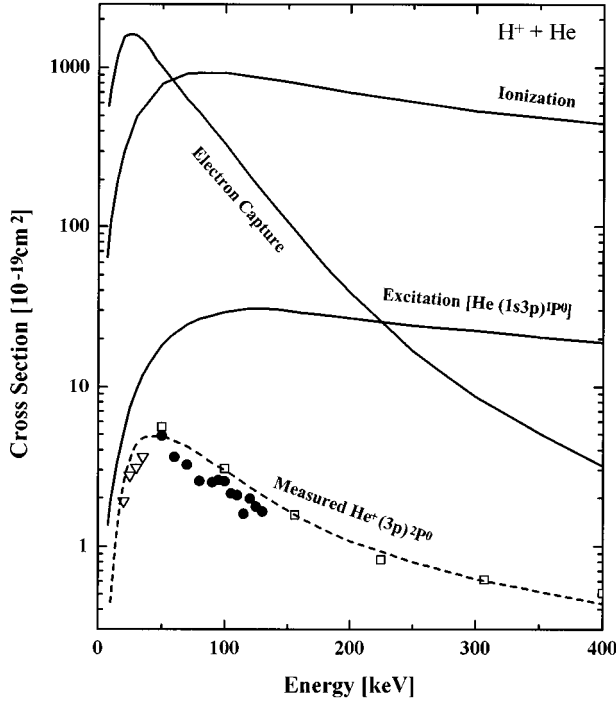


FIG. 3. Variation of cross sections for the production of $\text{He}^+ (3p) {}^2P^\circ$ with projectile energy. The ionization [25], total electron capture [11], and excitation cross sections for $\text{He} (1s3p) {}^1P^\circ$ [22–24] are included for comparison. The heavy dashed line passing through the measured, excited He^+ data represents a linear combination of the various cross-section products for excitation, ionization, and capture (see text). Present results, ●, cascade corrected, and those of Bailey *et al.* [2], □, and van Eck [15], ▽, neither of which have been corrected for cascade contributions, are included for comparison.

obtained by assuming target excitation to an excited He^+ ion following either electron capture or ionization processes. To obtain a rough estimate of the relative importance of these mechanisms the following simple model has been applied to assess the relative importance of ionization plus excitation and electron capture plus target excitation:

$$\sigma(\text{He}^+ (np) {}^2P^\circ) = A\sigma(\text{ionization})\sigma(\text{excitation}) + B\sigma(\text{ionization})\sigma(\text{capture}), \quad (4)$$

where A and B are fitting parameters. By choosing $A = 1.10 \times 10^{15} \text{ cm}^{-2}$ and $B = 5.76 \times 10^{14} \text{ cm}^{-2}$ (see the heavy dashed curve in Fig. 2) a reasonable representation of the measured energy dependence of the ionization excitation cross section is obtained. This estimate assumes that the mechanisms of ionization excitation and transfer excitation may both be described in terms of the independent-electron model [26]. In this model electron-electron correlation is ignored, thus allowing the cross sections (or probabilities) to be determined separately for each single-electron process and then combined to form the multielectron process. In order to understand the collision dynamics in more detail, more complex calculations including three-body Coulomb interactions are needed. Nevertheless, this simple model suggests that the dominant process at lower energies may be electron

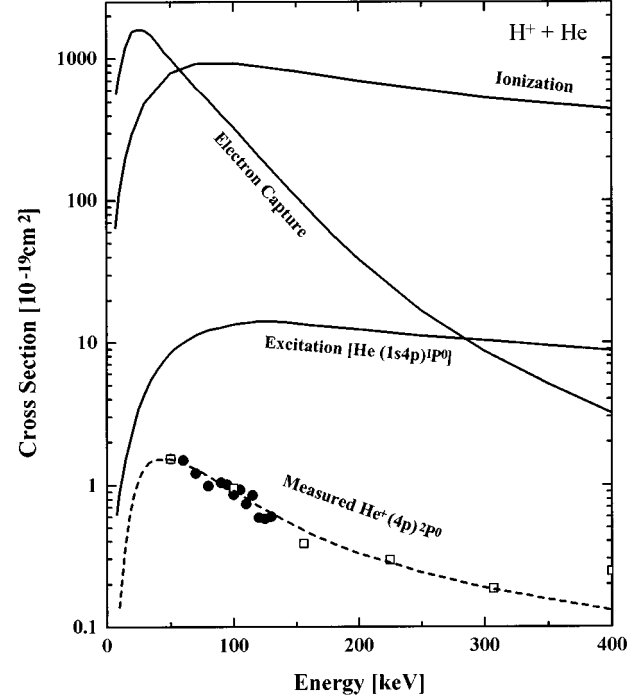


FIG. 4. Variation of cross sections for the production of $\text{He}^+ (4p) {}^2P^\circ$ with projectile energy. The ionization [25], total electron capture [11], and excitation cross sections for $\text{He} (1s4p) {}^1P^\circ$ [22–24] are included for comparison. The heavy dashed line passing through the measured, excited He^+ data represents a linear combination of the various cross-section products for excitation, ionization, and capture (see text). Present results, ●, cascade corrected, and those of Bailey *et al.* [2], □, are included for comparison.

capture plus excitation, with the ionization-plus-excitation process being dominant at higher impact energies. This conclusion is supported by a similar analysis extended to higher Rydberg levels with $A = 5.00 \times 10^{14} \text{ cm}^{-2}$, $B = 5.31 \times 10^{13} \text{ cm}^{-2}$ for $n=3$, and $A = 3.27 \times 10^{14} \text{ cm}^{-2}$, $B = 1.66 \times 10^{13} \text{ cm}^{-2}$ for $n=4$ (see heavy dashed curves in Figs. 3 and 4).

At present there is a great theoretical interest in the role of electron-electron correlation in such few-body processes [1,5–11], and in particular at threshold [27–31]. Therefore, theoretical studies of such correlated few-body processes are needed, along with further experiments involving different projectile ions. Multiply charged ion projectiles would also be of particular interest since they carry considerable potential energy into the collision system.

ACKNOWLEDGMENTS

We are indebted to Professor R. Phaneuf, Professor P. L. Altick, Dr. A. Franz, and M. Bailey from the University of Nevada, Reno for valuable comments. Furthermore, we would like to thank Dr. F. J. deHeer from the FOM Institute, The Netherlands, for providing copies of several difficult to get dissertations and journal articles. Finally, we are indebted to Dr. D. Dietrich from the Lawrence Livermore National Laboratory for providing us with an additional grating for our 2.2-m grazing incidence monochromator.

- [1] J. McGuire, *Advances in Atomic, Molecular, and Optical Physics* (Academic, New York, 1992), pp. 217–323.
- [2] M. Bailey, R. Bruch, E. Rauscher, and S. Bliman, *J. Phys. B* **28**, 2655 (1995).
- [3] K-H. Schartner, B. Lommel, and D. Detleffsen, *J. Phys. B* **24**, L13 (1991).
- [4] M. R. H. Rudge, *J. Phys. B* **21**, 1887 (1988).
- [5] S. Fülling, R. Bruch, E. A. Rauscher, P. A. Neill, E. Trabert, P. H. Heckmann, and J. H. McGuire, *Phys. Rev. Lett.* **68**, 3152 (1992).
- [6] J. O. Pedersen and F. Folkmann, *J. Phys. B* **23**, 441 (1990).
- [7] A. L. Ford and J. F. Reading, *Z. Phys. D* **21**, S241 (1991).
- [8] A. Franz and P. L. Altick, *J. Phys. B* **25**, L257 (1992).
- [9] A. V. Kuplyauskene and A. A. Maknitskas, *Opt. Spectrosc.* (USSR) **71**, 127 (1991).
- [10] R. A. Mapleton, *Phys. Rev.* **109**, 1166 (1952).
- [11] N. Stolterfoht, *Phys. Scr.* **42**, 192 (1990).
- [12] C. F. Barnett, Oak Ridge National Laboratory Report No. ORNL-6086/VI, 1990 (unpublished).
- [13] F. J. DeHeer, R. Hoekstra, and H. P. Summers, Jet Joint Undertaking, Report No. Jet-P(92)10, 1992 (unpublished).
- [14] R. K. Janev, *Comments At. Mol. Phys.* **26**, 83 (1991).
- [15] J. van Eck, Ph.D. thesis, Gemeente Universiteit, Amsterdam, 1964 (unpublished).
- [16] R. Bruch, E. A. Rauscher, S. Fülling, D. Schneider, S. Mannervik, and M. Larsson, *Encyclopedia of Applied Physics* (AIP, New York, 1994), Vol. 10, pp. 437–470.
- [17] E. W. Thomas, *Excitation in Heavy Particle Collisions* (Wiley, New York, 1972), pp. 6–162.
- [18] S. Fülling and R. Bruch, *Nucl. Instrum. Methods B* **79**, 779 (1993).
- [19] G. Liu, S. Fülling, and R. Bruch, *Comput. Phys.* **6**, 168 (1992).
- [20] J. T. Morgan, J. Geddes, and H. B. Gilbody, *J. Phys. B* **6**, 2118 (1973).
- [21] R. K. Janev and P. S. Krstic, *Phys. Rev. A* **46**, 5554 (1992).
- [22] M. Bailey, R. Bruch, E. Rauscher, and S. Bliman (unpublished).
- [23] W. C. Stolte, Ph.D. thesis, University of Nevada, Reno, 1994 (unpublished).
- [24] John T. Park and F. D. Schowengerdt, *Phys. Rev.* **185**, 152 (1969).
- [25] M. E. Rudd, Y.-K. Kim, D. H. Madison, and J. W. Gallagher, *Rev. Mod. Phys.* **57**, 965 (1985).
- [26] V. A. Sidorovich, V. S. Nikolaev, and J. H. McGuire, *Phys. Rev. A* **31**, 2193 (1985).
- [27] J. H. Macek, *Bull. Am. Phys. Soc.* **40**, 1327 (1995).
- [28] S. Watanabe, *Bull. Am. Phys. Soc.* **40**, 1327 (1995).
- [29] M. Pieksma and C. C. Havener, *Bull. Am. Phys. Soc.* **40**, 1323 (1995).
- [30] M. Pieksma and S. Y. Ovchinnikov, *J. Phys. B* **27**, 4573 (1994).
- [31] M. Pieksma *et al.*, *Phys. Rev. Lett.* **73**, 46 (1994).